Structure and Band-Gap Design of a New Series of Light-Emitting Poly(cyanofluorene-*alt*-*o*/*m*/*p*-phenylenevinylene)-Based Copolymers for Light-Emitting Diodes

Prasad Taranekar,[†] Mansour Abdulbaki,[‡] Ramanan Krishnamoorti,[‡] Sukon Phanichphant,[§] Paralee Waenkaew,[†,§] Derek Patton,[†] Timothy Fulghum,[†] and Rigoberto Advincula*[,†,‡]

Department of Chemistry and Department of Chemical Engineering, University of Houston, Houston, Texas 77204-5003, and Department of Chemistry, Chiang Mai University, Chiang Mai, Thailand

Received February 2, 2006; Revised Manuscript Received March 29, 2006

ABSTRACT: A new series of 2,2′-(9,9-dioctyl-9*H*-fluorene-2,7-diyl)diacetonitrile-based alternating polyfluorene copolymers (**P12-FL**, **P13-FL**, **P14-FL**) containing ortho-, meta-, and para-substituted phenylene derivatives have been designed, synthesized, and characterized. These polymers were synthesized using a Knoevenagel condensation polymerization reaction and were found to be predominantly in the trans configuration. The resulting polymers were found to be thermally stable and readily soluble in common organic solvents. The structural, configurational, and conformational changes in the backbone caused a wide variation in the absorption and emission maxima of the polymers. The fabricated light-emitting devices showed very good performance in terms of turn-on voltage, electroluminescence, and lifetime properties.

Introduction

Fluorescent conjugated polymers have attracted much attention due to their potential applications in flat panel displays.[1] Extensive research has been performed to develop highly efficient light-emitting polymers with tunable emission, long lifetimes, and color purity.[2] Presently, conjugated polymers are used for a variety of optoelectronic applications such as light-emitting diodes,[3] photovoltaic devices,[4] and field-effect transistors.[5] A wide range of polymers, such as poly(*p*-phenylenevinylene) (PPV), polythiophene (PT), poly(*p*-phenylene) (PPP), polyfluorene (PF), and their derivatives, have been extensively investigated as emissive materials.[6] Fluorene-based polymers are typically highly fluorescent in blue color, which is a required property for practical LED display applications.[7] The interest in these polymers arose because they exhibit high photoluminescence quantum yields and excellent chemical and thermal stability for a blue emitter. These materials are also known to have good photostability and film-forming properties and can be readily prepared via high-yielding synthetic routes that produce well-defined soluble high molecular weight polymers.[8]

The usefulness of PFs, however, is compromised by their tendency to exhibit excimer or aggregate formation and low electron affinity.[9] Therefore, it is a major challenge to design suitable PF polymers with low aggregation tendencies and improved electronic properties in terms of balanced charge-carrier transport. The intrinsic optoelectronic properties of a conjugated polymer are primarily governed by the chemical structure of the polymer backbone. Many different conjugated polymers have been investigated, and on the basis of these studies, it seems that chromic phenomena can be driven by a delicate balance between the steric hindrance created by the side groups along the backbone and attractive interchain (or intrachain, through chain folding) interactions.[10] Alternatively, such changes can also be achieved by adding suitable electron-donating or electron-withdrawing functional groups or altering the backbone conformation of the polymer main chain. Alteration in the backbone conformation can cause changes in the chain packing and film morphology, a macroscopic property, which can strongly affect the performance of conjugated polymer-based devices.[11] To form emissive excitons, high carrier density and mobilities are required, which requires a large degree of π-interactions between the polymer chains.[12] Once the carrier recombine and exciton is formed, however, minimal interchain contact is required to achieve the highest luminescence efficiency (and therefore the performance of PLEDs) which eventually depends on the way polymer chains are packed together by design.[13] On the other hand, altering the chemical structure allows fine-tuning of the highest occupied molecular orbital (HOMO) and the lowest unoccupied molecular orbital (LUMO) energy levels. Balancing these properties will ultimately affect the charge transport characteristics of the materials for optimum device performance.[14] This results in a fundamental tradeoff in optimizing polymer geometry and morphology for light-emitting applications.

To highlight this tradeoff in properties, copolymers of phenylene and fluorene vinylene units have been investigated by us. In the case of poly(phenylenevinylene), when phenylene units are replaced with fluorene units, the HOMO−LUMO gap is predicted to increase. The replacement does not change the HOMO energy level but lifts the LUMO energy level. To compensate this effect and reduce the band gap, cyano (CN) groups can be introduced on the fluorene units instead of the phenylene units. The cyano groups are also known to reduce the barrier to electron injection.[17] Thus, by altering these chemical structures and modifying the polymer backbone conformation, one can easily tune the electrooptical properties for this copolymer design. By simply changing the backbone structure and conformation, one can easily tune the color of emission as seen from Figure 1.

[†] Department of Chemistry, University of Houston.
[‡] Department of Chemical Engineering, University of Houston.
[§] Chiang Mai University.

10.1021/ma060253y CCC: $33.50
Published on Web 05/06/2006

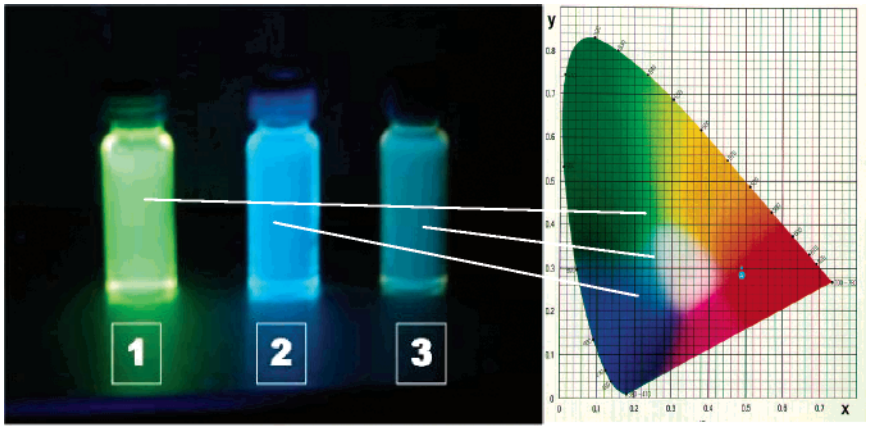

Figure 1. Solutions of **P14-FL** (**1**), **P13-FL** (**2**), and **P12-FL** (**3**) showing their distinct emission colors under UV irradiation with respect to a color chromaticity chart.

Scheme 1. Synthetic Routes to the Monomers

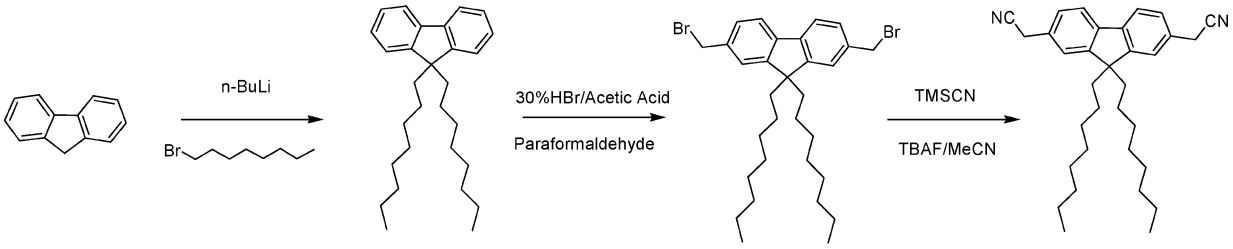

Specifically in this study, we report a series of cyanofluorene-alternating copolymers: poly[3-(4-(2-cyano-2-(7-methyl-9,9-dioctyl-9*H*-fluoren-2-yl)vinyl)phenyl)bis(methylacrylonitrile)] **(P14-FL)**, poly[3-(3-(2-cyano-2-(7-methyl-9,9-dioctyl-9*H*-fluoren-2-yl)vinyl)phenyl)bis(methylacrylonitrile)] **(P13-FL)**, poly-[3-(2-(2-cyano-2-(7-methyl-9,9-dioctyl-9*H*-fluoren-2-yl)vinyl)-phenyl)bis(methylacrylonitrile)] **(P12-FL)** containing para (p)-, meta (m)-, and ortho (o)-substituted phenylene derivatives, respectively. Previously, the results from a processable poly-(fluorene-*alt*-cyanophenylenevinylene), poly(cyanoterephthalylidene) (CN-PPV), and dialkoxy-substituted PPV derivative with cyano groups on the vinylene units have demonstrated improved device efficiency which was attributed to better electron injection facilitated by the electron-withdrawing cyano groups.[15] To our knowledge, this is the first report of a conformational polymer series based on an alternating fluorene−cyanophenylenevinylene, exhibiting large changes in photophysical behavior and device performance within a series (Scheme 2). While the use of the different phenylene substitutions (ortho, meta, para) seemed obvious, given the fact that the PPV series is one of the most well-studied polymers, no reports have yet appeared on this combination with fluorenes. This substitution pattern, as will be described later, changes the photophysical and device performance dramatically. A careful analysis of the structure−property relationships in this class of materials should lead to a better understanding of the rational design of new chromic conjugated polymers.

Experimental Section

Instrumentation. ^{1}H and ^{13}C NMR spectra were recorded on a General Electric QE 300 spectrometer (300 MHz). UV−vis was recorded using an Agilent 8453 spectrometer. Fluorescence spectra were obtained using a Perkin-Elmer LS45 luminescence spectrometer. The SEC analysis was performed using a Viscotek 270 quad detector equipped with UV−vis, refractive index, right-angle light scattering, and viscometry detectors. The columns used were Viscogel G3000H_{HR} and GHM_{HR}-M. FTIR measurements were done using a Digilab FTS 7000 (Varian) spectrometer. The thermal properties of the polymers and copolymers were measured on a TA Instruments 2050 thermogravimetric analyzer (TGA). Cyclic voltammetry (CV) was performed on an Amel 2049 potentiostat and power lab/4SP system with a three-electrode cell.

Device Fabrication/Testing. Indium tin oxide (ITO)-coated glass was obtained from SPI Supplies with an initial resistance of ~0.3 ohm. After cutting (1 × 1 in. squares), the ITO pieces were sonicated sequentially for 15 min in 2% sonicating solution, water, acetone, and 2-propanol. The ITO was then covered with two strips of Scotch brand tape as a mask against acid etching, which was conducted by placing the slides in a solution of 1:1 H_2O and HCl for 20 min. After etching, the substrates were sonicated for 15 min in DI water, acetone, and 2-propanol. The substrates were then plasma cleaned under oxygen for 5 min. PEDOT/PSS solution was obtained from Bayer Corp. and filtered through a 0.2 μm syringe filter prior to use. The PEDOT/PSS solution was spin-coated at 1000 rpm using a Speedline Technologies P6204 spin-coater. After drying the PEDOT/PSS-coated substrates for 2 h in a vacuum oven at 50 °C, each of the polymers (**P12-FL**/**P13-FL**/**P14-FL**) was then spin-coated at 1000 rpm, maintaining a thickness of ca. 90 nm. The polymer solutions were at 1.9 mg/mL concentration in distilled anhydrous toluene. The substrates were placed under vacuum with no heat for 1 h. Thermal evaporation of aluminum was done below 10^{-6} Torr using an Edwards E306 thermal evaporator. The active sections of the devices were then covered with an epoxy resin and allowed to dry so that the active regions were shielded from oxygen exposure during device testing. The devices were tested using a Keithley 236 source meter unit, a Hamamatsu photonics photomultiplier, and a home-written Lab-View program. Current−voltage−luminescence data were collected from 0 to 10 V at steps of 0.10 V. EL lifetime measurements were done under a constant potential of 8 V.

Reagents. The solvents used were properly distilled and collected immediately before any reaction or measurement. All other reagents were analytical grade, purchased commercially from Aldrich

Scheme 2. Synthetic Routes to Polymers: P14-FL, P13-FL, and P12-FL

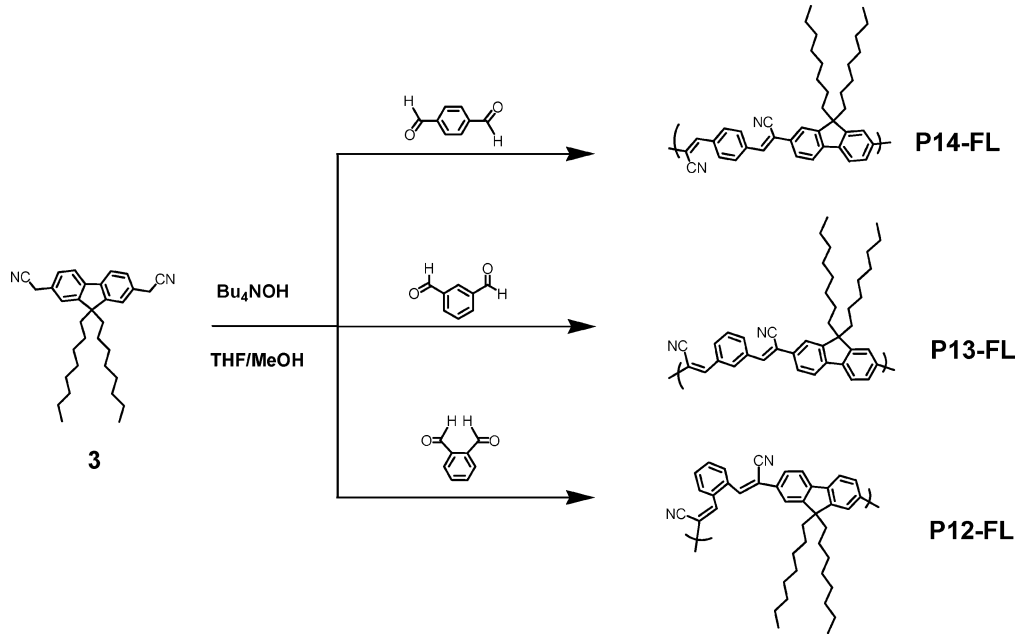

Chemical Co. and used without further purification. ITO was used as a working electrode and was pretreated with RCA recipe (H_2O/H_2O_2/NH_3: 15.1 g/26.6 g/8.57 g). 9,9-Dioctyl-9*H*-fluorene (**1**) was prepared as previously reported.[16]

Synthesis of 2,7-Bis(bromomethyl)-9,9-dioctyl-9*H*-fluorene (2) (Scheme 1). A mixture of 4 g (10.4 mmol) of 9,9-dioctyl-9*H*-fluorene (**1**), 3.2 g (106 mmol) of paraformaldehyde, and 7.2 mL of 30% concentrated hydrogen bromide in acetic acid was stirred at 80 °C for 24 h. After cooling to room temperature, the reaction mixture was slowly poured into saturated $NaHCO_3$ solution, extracted with CH_2Cl_2, and washed with water and brine. The combined extract was dried over Na_2SO_4. After removal of the solvent, the crude product was purified by column chromatography using petroleum ether as an eluent to obtain **2** in 65% yield. ^{1}H NMR ($CDCl_3$): δ (ppm) 0.80 (t, 6H), 1.0−1.07 (m, 20H), 1.95 (m, 4H), 4.60 (s, 4H), 7.28−7.30 (s, 2H), 7.34−7.43 (m, 2H), 7.64 (m, 2H). ^{13}C NMR ($CDCl_3$): δ (ppm) 14.0, 22.5, 23.6, 29.1, 29.13, 29.8, 31.7, 35.2, 55.1, 40.1, 119.9, 123.2, 127.5, 136.9, 140.7, 151.6.

Synthesis of 2,2′-(9,9-Dioctyl-9*H*-fluorene-2,7-diyl)diacetonitrile (3) (Scheme 1). To a stirred solution of 1.5 g (2.88 mmol) of 2,7-bis(bromomethyl)-9,9-dioctyl-9*H*-fluorene (**2**) in 30 mL of acetonitrile at room temperature under nitrogen were added 1.16 mL (8.64 mmol) of trimethylsilyl cyanide and 8.60 mL (8.64 mmol) of tetrabutylammonium fluoride (TBAF), and the reaction mixture was stirred for 12 h. The light yellow reaction mixture was concentrated under reduced pressure. The oily residue was purified by flash chromatography using ethyl acetate:hexane (1:10) to give compound **3** in 90% yield as a white solid. ^{1}H NMR ($CDCl_3$): δ (ppm) 0.40−0.61 (m, 4H), 0.77 (t, 6H), 1.0−1.20 (m, 20H), 1.90−1.96 (m, 4H), 3.80 (s, 4H), 7.25 (d, 4H), 7.62 (d, 2H). ^{13}C NMR ($CDCl_3$): δ (ppm) 14.04, 22.57, 23.79, 29.17, 29.86, 31.74, 40.18, 55.78, 117.89, 120.41, 122.04, 125.39, 129.72, 140.58, 152.31.

Synthesis of Poly[3-(4-(2-cyano-2-(7-methyl-9,9-dioctyl-9*H*-fluoren-2-yl)vinyl)phenyl)bis(methylacrylonitrile)] (P14-FL) (Scheme 2). To a stirred solution of 225 mg (0.48 mmol) of **3** and 64.3 mg (0.48 mmol) of terephthalaldehyde in 25 mL of THF and 12 mL of MeOH at reflux (65 °C) under nitrogen was added 0.30 mL of Bu_4NOH in methanol (1 M). After refluxing for 12 h, the reaction mixture was treated with 30 mL of MeOH and cooled to 0 °C over 15 min. The resulting solid obtained was then filtered off and purified by Soxhlet extraction with methanol to generate an orange solid in 68.5% yield. ^{1}H NMR ($CDCl_3$): δ (ppm) 0.63 (b, 4H), 0.77−0.82 (b, 6H), 1.07−1.29 (b, 20H), 2.07 (b, 4H), 6.96 (b, 1H), 7.60−7.81 (b, 7H), 7.73−7.99 (b, 2H), 8.0−8.11 (b, 2H). ^{13}C NMR ($CDCl_3$): δ (ppm) 14.04, 22.57, 23.79, 29.17, 29.86, 31.74, 40.18, 55.78, 113.5, 117.89, 120.41, 120.77, 125.4, 127.49, 127.59, 129.72, 130.31, 137.2, 140.58, 152.31.

Synthesis of Poly[3-(3-(2-cyano-2-(7-methyl-9,9-dioctyl-9*H*-fluoren-2-yl)vinyl)phenyl)bis(methylacrylonitrile)] (P13-FL) (Scheme 2). Polymer **P13−FL** was synthesized using a similar procedure as described for **P14-FL**. 225 mg (0.48 mmol) of **3** and 64.3 mg (0.48 mmol) of isophthalaldehyde were used to finally obtain a yellow solid in 80% yield. ^{1}H NMR ($CDCl_3$): δ (ppm) 0.64 (b, 4H), 0.77−0.82 (b, 6H), 1.07−1.29 (b, 20H), 2.09 (b, 4H), 7.60−7.69 (b, 6H), 7.73−7.76 (b, 2H), 7.81−7.84 (b, 1H), 8.06−8.09 (b, 2H), 8.32 (b, 1H). ^{13}C NMR ($CDCl_3$): δ (ppm) 14.04, 22.57, 23.79, 29.17, 29.86, 31.74, 40.18, 55.78, 113.5, 117.89, 120.41, 120.77, 125.4, 129.72, 130.31, 130.54, 134.69, 140.58, 141.6, 152.31.

Synthesis of Poly[3-(2-(2-cyano-2-(7-methyl-9,9-dioctyl-9*H*-fluoren-2-yl)vinyl)phenyl)bis(methylacrylonitrile)] (P12-FL) (Scheme 2). Polymer **P12-FL** was also synthesized using a similar procedure as described for **P14-FL**. 225 mg (0.48 mmol) of **3** and 64.3 mg (0.48 mmol) of phthalaldehyde were used to finally obtain a red solid in 50% yield. ^{1}H NMR ($CDCl_3$): δ (ppm) 0.62 (b, 4H), 0.77−0.87 (b, 6H), 1.07−1.27 (b, 20H), 1.95 (b, 4H), 6.91−7.89 (b, 10H), 8.06−8.24 (b, 2H). ^{13}C NMR ($CDCl_3$): δ (ppm) 14.04, 22.57, 23.79, 29.17, 29.86, 31.74, 40.18, 55.78, 113.5, 117.89, 120.41, 120.77, 125.39, 126.3, 127.9, 129.72, 137.9, 138.71, 130.86, 140.58, 152.31.

Results and Discussion

Synthesis and Characterization. The syntheses of the monomers and polymers are outlined in Scheme 1 and Scheme 2. After accomplishing the reported synthesis of 9,9-dioctyl-9*H*-fluorene (**1**), it was then converted to 2,7-bis(bromomethyl)-9,9-dioctyl-9*H*-fluorene (**2**) using 30% concentrated hydrogen bromide and paraformaldehyde. Compound **2** was then converted to 2,2′-(9,9-dioctyl-9*H*-fluorene-2,7-diyl)diacetonitrile (**3**) using TMSCN/TBAF. The synthesis of compound **3** is more efficient in terms of reaction time and yield by using TMSCN/TBAF reagents as compared to the use of NaCN. Compound **3** was then further reacted with terephthalaldehyde/isophthalaldehyde/phthalaldehyde to give **P14-FL**/**P13-FL**/**P12-FL** polymers, respectively, using the Knoevenagel condensation method. The polymers were found to be readily soluble in common organic solvents such as THF, CH_2Cl_2, $CHCl_3$, toluene, and xylene. The polymers were dissolved in THF, and the molecular

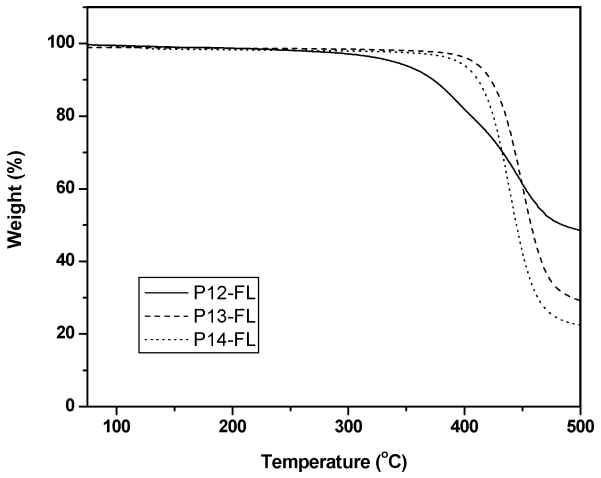

Figure 2. Thermogravimetric analysis of the polymers under N_2.

Table 1. Number-Average (M_n) and Weight-Average (M_w) Molecular Weights and Thermal Properties of the Polymers

polymers	M_n	M_w	M_w/M_n	TGA (onsets), °C
P12-FL	3487	5180	1.48	322
P13-FL	11543	35925	3.11	398
P14-FL	8228	19665	2.39	391

weight was determined using gel permeation chromatography (GPC) against polystyrene standards. The molecular weights of the polymers are summarized in Table 1. Although not very high molecular weights were achieved, the range was found consistent with previously reported literature on CN-poly(fluorenevinylene) using the Knoevenagel reaction.[17] The polydispersity of these polymers was found to increase though with increasing molecular weight. While high MWs have been achieved for a variety of conjugated polymers, some of the more interesting electrooptical properties have been observed with low-MW conjugated polymer derivatives.[12d] In principle, the differences in molecular weight can be correlated with the relative chain stiffness by calculating or estimating Mark−Houwink (α) constant.[17c] The chain stiffness, which reflects the polymer chain conformation in solution, could be affected by the conjugation length and the extent of the trans configuration within these copolymers. **P12-FL** is expected to have a tendency for helical conformation because of torsional strain and an earlier break in conjugation sequences. **P14-FL** is expected to have the highest conjugation length and at the same time a larger extent of trans character, increasing the chain rigidity and stiffness. **P13-FL** is expected to fall in between both these parameters and therefore should have the lowest (α) value, indicating highest chain flexibility and a broken conjugation due to meta inclusion in the polymer backbone. These configurational/conformational differences can be clearly observed in a structural modeling of their oligomeric sequences (see Supporting Information). As such, the resulting differences in conjugation length directly affect the electrooptical properties as will be observed in the subsequent results and discussions. This chain stiffness factor can ultimately dictate polymer chain packing and film properties and can be further investigated by detailed X-ray analyses and light scattering studies in solution.

The thermal properties of the polymers were evaluated by means of TGA as seen from Figure 2. The samples were heated to 800 °C at a heating rate of 10 °C/min under a dry nitrogen atmosphere. The weight loss of the polymers was less than 10% upon heating to 400 °C, indicative of good thermal stability. The onset of thermal degradation is also summarized in Table 1.

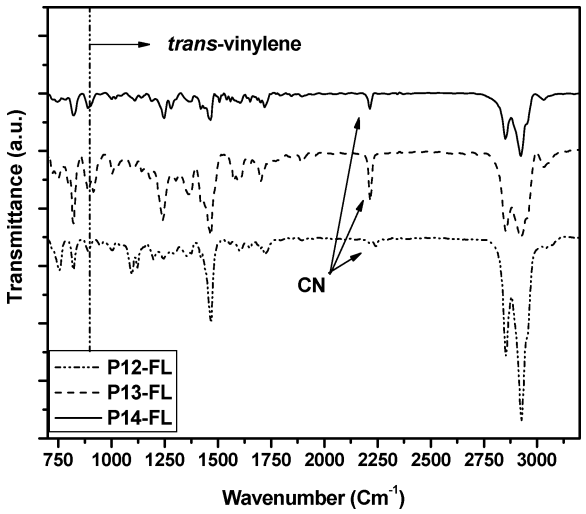

Figure 3. FT-IR transmission spectra of the polymer series in KBr.

FTIR Studies.[18] FT-IR spectra of the polymers are shown in Figure 3. The FTIR studies clearly suggest the conformational differences based upon the out-of-plane (C−H) wag vibration frequencies, which appear at 750/782/817 cm^{-1} corresponding to o/m/p-disubstituted positions, respectively. The band at 1470 cm^{-1} appears to be due to disubstituted aromatic C−H vibration. This vibration is also observed at 3050 cm^{-1} and is more prominent in meta-disubstituted aromatic compounds.

The peak at 905 cm^{-1} is assigned to the out-of-plane stretch of *trans*-vinylene, suggesting that the copolymers are predominantly in the trans configuration. The C═C frequencies arising from out-of-plane olefin hydrogen wag vibrations also occurs at 1730 cm^{-1}, which is slightly higher due to the presence of electron-withdrawing cyano groups. The cyano groups exhibit a medium-intensity, sharp band in the triple-bond region of the spectrum (2270−2210 cm^{-1}), and conjugation with double bonds or aromatic rings moves this absorption to a lower frequency. As a result, the stretch absorption band due to cyano groups in the polymers appears typically at 2216 cm^{-1} for these series. The lower intensities of the cyano group for **P12-FL** relative to the aromatic C−H band can be explained by a stronger dipole−dipole interaction between the cyano groups. This does not seem to be the case for **P13-FL** and **P14-FL** perhaps due to its backbone geometry (Supporting Information). Unlike the two polymers which have a more linear structure, the **P12-FL** is the most twisted due to the ortho substitution pattern. The nature of this dipole−dipole interaction should therefore be intramolecular in nature. The meta-substituted **P13-FL** has the highest intensity for the cyano frequency, indicating less dipole−dipole interaction.[15] The dipole−dipole interactions of the cyano groups is crucial since it decreases the electron-withdrawing nature of the cyano group and thereby affect the band-gap behavior of these polymers.

Optical and Photoluminescence Properties. Figure 4a shows the optical absorption and PL spectra of polymers, **P12-FL**, **P13-FL**, and **P14-FL** in 10^{-5} M THF solution. Figure 4b shows the polymer solid-state spectra taken after spin-coating individual polymer thin films on indium tin oxide (ITO). The UV−vis of the copolymers in solution shows $\pi-\pi^*$ transitions of the polymer backbone occurring at 338, 388, and 425 nm and their corresponding PL peaks at 487, 445, and 516 nm for **P12-FL**, **P13-FL**, and **P14-FL**, respectively. This obvious relative spectral red shift, in both absorption and emission for this series of polymers, can be understood in terms of better conjugation as expected from the structural disparity and

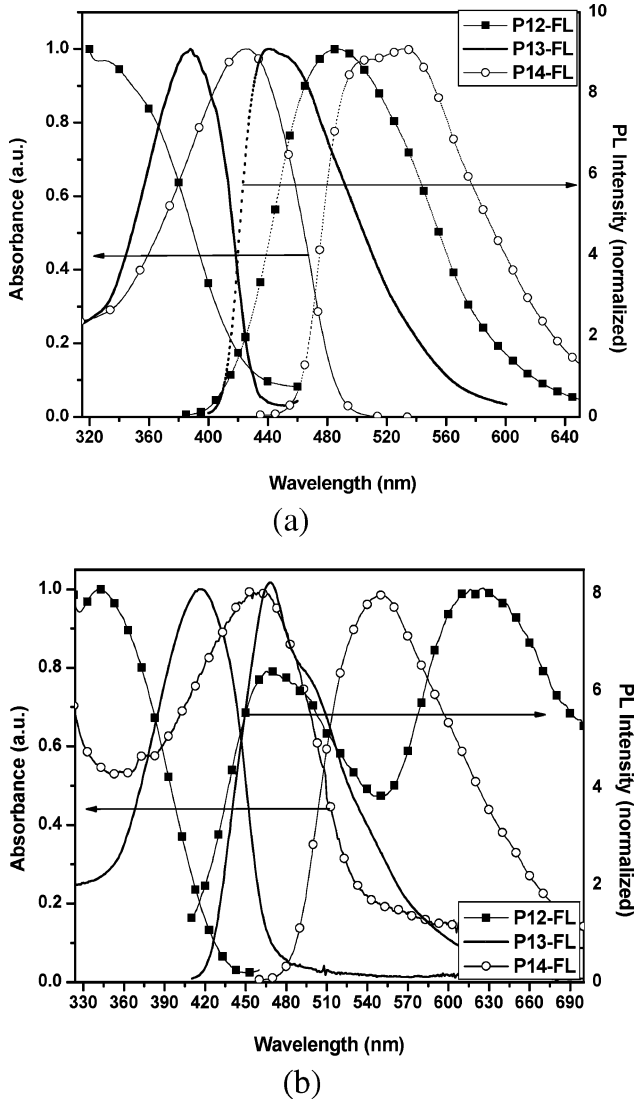

Figure 4. UV−vis and fluorescence spectra of polymers: (a) in 10^{-5} M THF solution; (b) spin-coated films on ITO.

introduction of the vinylene units in the backbone. The Stokes shift between the absorption and emission of these three polymers in solution were found to be 149, 57, and 96 nm, corresponding to **P12-FL**, **P13-FL**, and **P14-FL**, respectively. The smallest Stokes shift in the case of the **P13-FL** polymer would indicate a more favorable structure of the conjugated main chain leading to optimal ground−excited state energy transitions giving blue emission.[19] Whereas, in the case of **P14-FL**, there is more thermal energy loss and the emission is significantly shifted to the green.

Figure 4b shows the solid-state polymer $\pi-\pi^*$ transitions observed at 342, 416, and 457 nm, and their corresponding PL spectra occur at 469 and 621 nm for **P12-FL** polymer and at 468 and 547 nm for **P13-FL** and **P14-FL**, respectively. The PL peak at 621 nm for **P12-FL** can be attributed to the excimer-like adducts between photoexcited polymers and/or internal charge transfer along the polymer backbone in the solid state.[20] Once again the smallest Stokes shift value and sharp vibronic features are observed in the case of **P13-FL** polymer, which is similar to the case found in ladder-type poly(*p*-phenylene).[21] Although **P13-FL** shows a narrower spectrum at 468 nm, it begins to show peak broadening from 500 nm, indicating the presence of aggregation. This is expected from **P13-FL** on the basis of its structural configuration. On the other hand, a

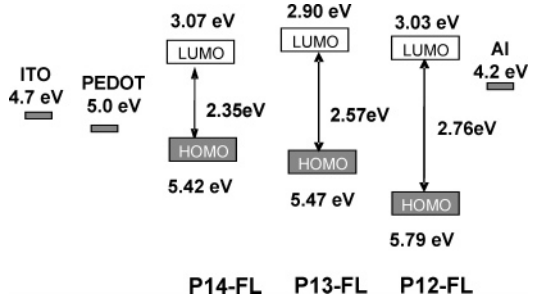

Figure 5. Energy band diagram of **P12-FL**, **P13-FL**, and **P14-FL** polymers.

relatively broad emission spectrum (547 nm) was observed for **P14-FL,** suggesting little or no aggregation in contrast to polyfluorenes.[7] This indicates the absence of conformational defects and less excimer formation due to aggregation in the case of **P14-FL**.

Electrochemical Studies. Cyclic voltammetry (CV) was employed to investigate the redox behavior of the polymers and to estimate their HOMO and LUMO energy levels. The polymer films were spin-coated onto ITO electrodes and scanned positively and negatively at a scan rate 100 mV/s in a 0.1 M solution of tetrabutylammonium perchlorate (Bu_4NClO_4) in anhydrous acetonitrile. In the anodic scan, the onsets of oxidation of **P12-FL**, **P13-FL**, and **P14-FL** were found to occur at 1.4, 1.08, and 1.03 V (Vs Ag/Ag^+), which correspond to the ionization potentials (Ip) −5.79, −5.47, and −5.42 eV, respectively, according to the empirical relationships proposed by Leeuw et al.:[22]

$$(\mathrm{Ip(HOMO)}) = -(E_{\mathrm{onset,ox}} + 4.39)\ (\mathrm{eV}),$$
$$E_{\mathrm{a}}(\mathrm{LUMO})) = -(E_{\mathrm{onset,red}} + 4.39)\ (\mathrm{eV})$$

where $E_{\mathrm{onset,ox}}$ and $E_{\mathrm{onset,red}}$ are the onset potentials of oxidation and reduction, respectively. In the cathodic scan, the LUMO energy levels for **P12-FL**, **P13-FL**, and **P14-FL** are determined to be −1.36 V (−3.03 eV), −1.49 V (−2.90 eV), and −1.32 V (−3.07 eV). The cyano group on the polymers is responsible for lowering the LUMO levels (3.03−3.07 eV), although these values are higher than those of poly(fluorenevinylene) (2.6 eV) and MEH−PPV (2.1 eV).[17b] This implies that the polymers should have improved electron injection and transport properties.

The energy band gaps, which can be calculated from the HOMO/LUMO energy levels, for **P12-FL**, **P13-FL**, and **P14-FL** were found to be 2.76, 2.57, and 2.35 eV, respectively (Figure 5). As in the cathodic scan, the anodic scans were found to be less sensitive, but both of these scans were irreversible in nature.

The optical energy onsets closely matched their respective electrochemical energy band gaps. The optical bad gap onsets for **P12-FL**, **P13-FL**, and **P14-FL** were found to be 2.8 eV (450 nm), 2.59 eV (485 nm), and 2.38 eV (529 nm), respectively. The variation in the band gap energy level of the series is a result not only of the introduction of cyano groups, but also as a function of effective conjugation length caused by the structural changes in the backbone. For example, it is known that meta substitution shows a broken conjugation, and the degree of effective conjugation highly depends on the torsional strain across the backbone.[17c,23] The largest band gap in the case of **P12-FL** is due to a highly noncoplanar nature based on conformational twists of the backbone structure. The lowest band gap is with **P14-FL** is due to a more linear and conjugated polymer backbone as a result of the para substitution and trans

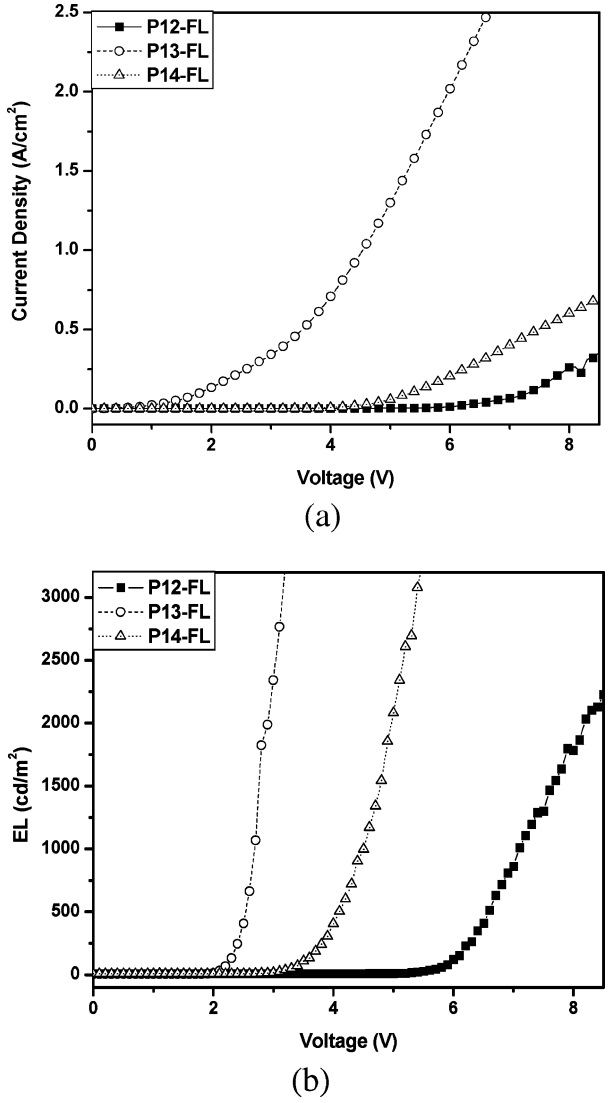

Figure 6. PLED studies for polymers: (a) current density−electric field ($I-V$) curves; (b) luminance−electric field ($EL-V$) curves.

configuration. On the other hand, **P13-FL** is in between (see Supporting Information).

Device Studies. Light-emitting diode devices were fabricated in order to test the current−voltage−luminescence and lifetime properties of the polymers to determine their viability for use in organic optoelectronic devices. On the basis of the band gap/energy level of the polymers, an ITO/PEDOT/PX-FL/Al multilayer device configuration was found suitable.

Though the difference in turn-on voltages will lead to a disparity in current density and brightness at a particular voltage, another attribute to consider would be the slopes of the $I-V$ and $EL-V$ curves. These are indicative of the rate at which the current and brightness are increasing. From Figure 6a,b, both current and electroluminescence vs voltage data exhibit readily observable increases in the slopes from **P12-FL** to **P14-FL** and **P13-FL**. A higher slope indicates either efficient charge injection, higher charge mobility, or a combination of both.

Figure 6a compares the $I-V$ curves for the double-layered diodes. With an increasing forward bias voltage, the current in all the devices increases, which is a typical rectifying characteristic. Both the polymers **P13-FL** and **P14-FL** show electroluminescence greater than 3000 cd/m^2, as seen from Figure 6b. The maximum luminous efficiency of the three polymers was found to be ca. 0.53 lm/W (0.73 cd/A) at 3 V for **P13-FL**,

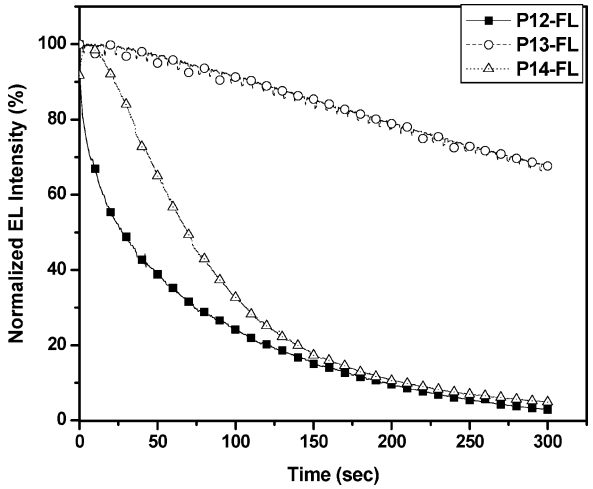

Figure 7. Electroluminescent lifetime data for the polymers fabricated with a configuration of ITO/PEDOT:PSS/P-FL polymer/Al.

Table 2. Original Brightness after 1 and 5 min and Sustainability Factor for the polymers

polymers	% of original brightness after 1 min	% of original brightness after 5 min	sustainability factor (τ)
P12-FL	35	3	99
P13-FL	96	68	714
P14-FL	57	05	215

1.96 lm/W (2.7 cd/A) at 5 V for **P14-FL**, and 0.087 lm/W (0.12 cd/A) at 7 V for **P12-FL**.

Several things can be noted on the basis of the device performance results. **P12-FL** exhibited the highest EL turn-on voltage at 6.4 V, followed by **P14-FL** at 4.1 V and the lowest with **P13-FL** at 2.4 V.

The difference in the turn-on voltage may be due to aggregation between conjugated polymer chromophores, which tend to promote good carrier transport through the film but at the same time reduce the luminescence efficiency via the formation of interchain species such as excimers or polaron pairs.[24,25] However, more detailed studies are underway to understand the disparity in turn-on voltage, which may be due to the morphological changes and the nature of interchain interaction. While no specific studies were made with film morphology for this series, it should be noted that differences in film properties eventually affects the luminescence quantum efficiency and device performance. Thus, this situation should eventually lead to a fundamental tradeoff paradigm between polymer morphology, i.e., chain packing and its band gap.[26,27]

Electroluminescent lifetimes of the devices were also tested with results following the same trend as with the other performance factors. Table 2 shows the decrease in brightness after 60 s of running at 8 V and after 5 min (600 s). The 60 s mark shows all three conformations performing well but with **P13-FL** polymer bearing a more resilient device structure.

Figure 7 shows a clear distinction in the lifetime extinction curves of the normalized device intensity. A sustainability factor (τ) can be extracted by fitting the extinction curves to an equation of the form $EL\ (\%) = L_0 \exp(-t/\tau)$, where t is time. Higher values of τ reduce the magnitude of the slope, indicating a higher electroluminescent sustainability and longer device lifetimes. Clearly the **P13-FL** polymer showed a more superior performance than the two other polymers. In which case, the low turn-on voltage, more efficient performance, and longer lifetime of this polymer indicate an optimal structure and band

gap design for this series of conjugated polymers in terms of LED applications.

Conclusions

In summary, a new series of processable polymers with cyanofluorene groups alternating with phenylenevinylene at ortho-, meta-, and para-substituted positions were synthesized and characterized. Optical and PL properties varied based on the structure and conformation of the polymer backbone. The optical energy onsets closely matched with their respective electrochemical energy band gaps. The PLED devices were fabricated to achieve emission of both green and blue light for **P14-FL** and **P13-FL** polymers, respectively. **P13-FL** was found to be more superior in having a low turn-on voltage of 2.4 V and the smallest Stokes shift value. At the same time **P14-FL** was found to show the highest luminous efficiency. While the required potential across each of these devices varies, the turn-on voltages of these copolymers are relatively low and show promise for viability of these materials in future display devices. More importantly, this work has emphasized the importance of chain structure and band gap design toward improved light-emitting materials. Future studies will focus on more in-situ film morphology characterizations.

Acknowledgment. The authors gratefully acknowledge the partial funding from the Robert E. Welch Foundation (E-1551), NSF DMR-0504435, DMR-99-82010, and Royal Golden Jubilee Scholarship of Thailand. We also acknowledge technical support from Varian Inc and from Viscotek Inc.

Supporting Information Available: Molecular structure modeling of the 2,2′-(9,9-dioctyl-9*H*-fluorene-2,7-diyl)diacetonitrile-based alternating polyfluorene copolymer (**P12-FL**, **P13-FL**, **P14-FL**) series. This material is available free of charge via the Internet at http://pubs.acs.org.

References and Notes

(1) (a) Wu, F. I.; Shih, P. I.; Shu, C. F.; Tung, Y. L.; Chi, Y. *Macromolecules* **2005**, *38*, 9028. (b) Kido, J.; Kimura, M.; Nagai, K. *Science* **1995**, *267*, 1332. (c) Wu, F. I.; Shih, P. I.; Tseng, Y. H.; Chen, G. Y.; Chien, C. H.; Shu, C. F.; Tung, Y. L.; Chi, Y.; Jen, A. K. Y. *J. Phys. Chem. B* **2005**, *109*, 14000.

(2) (a) Jin, S. H.; Jang, M. S.; Suh, H. S.; Cho, H. N.; Lee, J. H.; Gal, Y. S. *Chem. Mater.* **2002**, *14*, 643. (b) Chen, Y.; Araki, Y.; Doyle, J.; Strevens, A.; Ito, O.; Blau, W. J. *Chem. Mater.* **2005**, *17*, 1661. (c) Greenham, N. C.; Friend, R. H. *Solid State Phys.* **1996**, *49*, 1.

(3) (a) An, B. K.; Kim, Y. H.; Shin, D. C.; Park, S. Y.; Yu, H. S.; Kwon, S. K.; *Macromolecules* **2001**, *34*, 3993. (b) Burns, P. L.; Holmes, A. B.; Kraft, A.; Bradley, D. D. C.; Brown, A. R.; Friend, R. H.; Gywer, R. W. *Nature (London)* **1992**, *356*, 47.

(4) (a) Peng, K. Y.; Chen, S. A.; Fann, W. S. *J. Am. Chem. Soc.* **2001**, *123*, 11388. (b) Wohrle, D.; Meissner, D. *Adv. Mater.* **1991**, *3*, 129.

(5) (a) Kulkarni, A. P.; Tonzola, C. J.; Babel, A.; Jenekhe, S. A. *Chem. Mater.* **2004**, *16*, 4556. (b) Bao, Z.; Lovinger, A. J.; Brown, J. *J. Am. Chem. Soc.* **1998**, *120*, 207.

(6) (a) Kraft, A.; Grimsdale, A. C.; Holmes, A. B. *Angew. Chem., Int. Ed.* **1998**, *37*, 402. (b) Friend, R. H.; Gymer, R. W.; Holmes, A. B.; Burroughes, J. H.; Marks, R. N.; Taliani, C.; Bradley, D. D. C.; Dos Santos, D. A.; Bredas, J. L.; Logdlund, M.; Salaneck, W. R. *Nature* (*London*) **1999**, *397*, 121. (c) Bernius, M. T.; Inbasekaran, M.; O'Brien, J.; Wu, W. W. *Adv. Mater.* **2000**, *12*, 1737.

(7) (a) Klarner, G.; Davey, M. H.; Chen, W. D.; Miller, R. D. *Adv. Mater.* **1998**, *10*, 993. (b) Miteva, T.; Meisel, A.; Knoll, W.; Nothofer, H. G.; Scherf, U.; Muller, D. C.; Meerholz, K.; Yasuda, A.; Neher, D. *Adv. Mater.* **2001**, *13*, 565. (c) Kong, X.; Kulkarni, A. P.; Jenekhe, S. A. *Macromolecules* **2003**, *36*, 8992.

(8) (a) Pei, Q.; Yang, Y. *J. Am. Chem. Soc.* **1996**, *188*, 7416. (b) Jacob, J.; Zhang, J.; Grimsdale, A. C.; Müllen, K.; Gaal, M.; List, E. J. W. *Macromolecules* **2003**, *36*, 8240. (c) Cho, H. J.; Jung, B. J.; Cho, N. S.; Lee, J.; Shim, H. K. *Macromolecules* **2003**, *36*, 6704. (d) Beauprè, S.; Leclerc, M. *Adv. Funct. Mater.* **2002**, *12*, 192. (e) Shu, C. F.; Dodda, R.; Wu, F. I.; Liu, M. S.; Jen, A. K. Y. *Macromolecules* **2003**, *36*, 6698.

(9) (a) Kraft, A.; Grimsdale, A. C.; Holmes, A. B. *Angew. Chem., Int. Ed.* **1998**, *37*, 402. (b) Xia, C.; Advincula, R. *Macromolecules* **2001**, *34*, 5854.

(10) (a) Schwartz, B. J. *Annu. Rev. Phys. Chem.* **2003**, *54*, 141. (b) Leclerc, M.; Faid, K. *Adv. Mater.* **1997**, *9*, 1087. (c) McCullough, R. D. *Adv. Mater.* **1998**, *10*, 93.

(11) (a) Nguyen, T.-Q.; Schwatz, B. J. *J. Chem. Phys.* **2002**, *116*, 8198. (b) Ding, L.; Karasz, F. E.; Lin, Z.; Zheng, M.; Liao, L.; Pang, Y. *Macromolecules* **2001**, *34*, 9183.

(12) (a) Nguyen, T.-Q.; Martini, I.; Liu, J.; Schwartz, B. J. *J. Phys. Chem. B* **2001**, *104*, 237. (b) Wang, P.; Collison, C. J.; Rothberg, L. J. *J. Photochem. Photobiol. A.* **2001**, *144*, 63. (c) Xia, C.; Advincula, R. *Macromolecules* **2001**, *34*, 6922. (d) Mullen, K.; Wegner, G. *Electronic Materials: The Oligomer Approach*; Wiley: Weinheim, 1998.

(13) (a) Nguyen, T.-Q.; Kwong, R. C.; Thompson, M. E.; Schwartz, B. J. *Appl. Phys. Lett.* **2001**, *76*, 2454. (b) Chen, X. L.; Lovinger, A. J.; Bao, Z. N.; Sapjeta, *J. Chem. Mater.* **2001**, *13*, 1341. (c) Kim, J. *Pure Appl. Chem.* **2002**, *74*, 2031.

(14) (a) Renak, M. L.; Bartholomew, G. P.; Wang, S.; Ricatto, P. J.; Lachicotte, R. J.; Bazan, G. C. *J. Am. Chem. Soc.* **1999**, *121*, 7787. (b) Oelkrug, D.; Tompert, A.; Gierschner, J.; Egelhaaf, H.-J.; Hanack, M.; Hohloch, M.; Steinhuber, E. *J. Phys. Chem. B* **1998**, *102*, 1902. (c) Strehmel, B. A.; Sarker, M.; Malpert, J. H.; Strehmel, V.; Seifert, H.; Neckers, D. C. *J. Am. Chem. Soc.* **1999**, *121*, 1226.

(15) (a) Jin, S. H.; Kim, Y. M.; Koo, D. S.; Kim, Y. I.; Park, S. H.; Lee, K.; Gal, Y. S. *Chem. Mater.* **2004**, *16*, 3299. (b) Greenham, N. C.; Moratti, S. C.; Bradley, D. D. C.; Friend, R. H.; Holmes, A. B. *Science* **1993**, *365*, 628.

(16) Ranger, M.; Leclerc, M. *Can. J. Chem.* **1930**, *8*, 1571.

(17) (a) Jin, Y.; Ju, J.; Kim, J.; Lee, S.; Kim, J. Y.; Park, S. H.; Son, S.-M.; Jin, S.-H.; Lee, K.; Suh, H. *Macromolecules* **2003**, *36*, 6970. (b) Jin, S.-H.; Kang, Y.-S.; Kim, Y.-M.; Chan, Y. U. *Macromolecules* **2003**, *36*, 3841. (c) Pang, Y.; Li, J.; Hu, B.; Karasz, F. E. *Macromolecules* **1999**, *32*, 3946−3950.

(18) Colthup, N. B. *Intro To Infrared & Raman Spectroscopy*, 2nd ed.; Academic Press: New York, 1975.

(19) (a) Liu, B.; Yu, W. L.; Pei, J.; Liu, S. Y.; Lai, Y. H.; Huang, W. *Macromolecules* **2001**, *34*, 7932. (b) Lemmer, U.; Heun, S.; Mahrt, R. F. Scherf, U.; Hopmeir, M.; Seigner. U.; Gobel; Mullen, K.; Bassler, H. *Chem. Phys. Lett.* **1995**, *240*, 373.

(20) Ojha, U. P.; Krishnamoorthy, K.; Kumar, A. *Synth. Met.* **2003**, *132*, 279.

(21) Yang, S. C.; Graupner, W.; Guha, S.; Puschnig, P.; Martin, C.; Chandrasekhar, H. R.; Leising, G.; Ambrosch-Draxl, C.; Scherf, U. *Phys. Rev. Lett.* **2000**, *85*, 2388.

(22) (a) deLeeuw, D. M.; Simenon, M. M. J.; Brown, A. R.; Einerhand, R. E. F. *Synth. Met.* **1997**, *87*, 53. (b) Chen, Z. K.; Huang, W.; Wang, L. H.; Kang, E. T.; Chen, B. J.; Lee, C. S.; Lee, S. T. *Macromolecules* **2000**, *33*, 9015.

(23) (a) Hong, S. Y.; Kim, D. Y.; Kim, C. Y.; Hoffmann, R. *Macromolecules* **2001**, *34*, 6474.

(24) (a) Lee, S. H.; Jang, B. B.; Tsutsui, T. *Macromolecules* **2002**, *35*, 1356. (b) Shi, J.; Zheng, S. *Macromolecules* **2001**, *34*, 6571. (c) Conwell, E. M. *Phys. Rev. B* **1998**, *57*, 14200. (d) Yan, M.; Rothberg, L. J.; Kwock, E. W.; Miller, T. M. *Phys. Rev. Lett.* **1995**, *75*, 1992.

(25) Nguyen, T. Q.; Martini, I. B.; Liu, J.; Schwartz, B. J. *J. Phys. Chem. B* **2000**, *104*, 237.

(26) Scott, J. C.; Brock, P. J.; Salem, J. R.; Ramos, S.; Malliaras, G. G. *Synth. Met.* **2000**, *111*, 289.

(27) (a) Hsieh, B. R.; Yu, Y.; Forsythe, E. W.; Schaaf, G. M.; Feld, W. A. *J. Am. Chem. Soc.* **1998**, *120*, 231. (b) Halim, M.; Pillow, J. G.; Samuel, I. D. W.; Burn, P. L. *Synth. Met.* **1999**, *102*, 922.

MA060253Y